

Texture evolution in tape cast lead metaniobate

Benjamin Iverson, Hyun Jun Kim, Elliott Slamovich, Keith Bowman*

School of Materials Engineering, Purdue University, West Lafayette, IN 47907, United States

Received 18 April 2007; received in revised form 17 July 2007; accepted 27 July 2007

Available online 29 October 2007

Abstract

Lead metaniobate ceramics were tape cast with inclusions of acicular seed particles. The effects of seed particle concentration, slurry viscosity, and casting velocity on the shear behavior of the tape cast slurry were quantified based on a model using the ratio of pressure driven forces to viscous driven forces. Texture was quantified using a combination of X-ray diffraction with the Lotgering factor and neutron diffraction with Rietveld refinement. The shear behavior of the individual slurries was linked to the amount of texture that is induced from given slurry.

© 2007 Elsevier Ltd. All rights reserved.

Keywords: Tape casting; Lead metaniobate; PbNb_2O_6 ; Piezoelectrics; Texture

1. Introduction

Tape casting ceramic powders with inclusions of shaped seed particles is a convenient way to induce crystallographic textures. While highly anisotropic ceramics can be created in this way, most investigations in this area focus on either the seed particle shape or the concentrations of seed particles in the slurry.^{1–4} While these two parameters do influence the degree of preferred orientation developed, there are other parameters related to the slurry rheology and operating conditions of the tape casting process that may effect the degree of developed texture. In this paper, the relationship between the rheology of the tape casting slurry and the conditions of the casting process used will be examined in relation to the amount of preferred orientation induced in a tape cast lead metaniobate ceramic.

Recently, Kim and coworkers conducted a model for tape casting Newtonian fluids with several simplifying assumptions.⁵ They employed a parameter, Π , to quantify the ratio of pressure forces to viscous forces acting on a tape cast slurry during deformation under a doctor blade. Utilizing all process conditions and slurry viscosity, it is possible to calculate Π and estimate whether a casting operation will be dominated by pressure flow or shear flow. From Kim's work, Π is given by the equation:

$$\Pi = \frac{\Delta P H^2}{2\mu L U} \quad (1)$$

where ΔP is the pressure exerted by the slurry head ($\Delta P = \rho_{\text{slurry}} g H_{\text{slurry}}$), H is the blade gap used, μ is the slurry viscosity, L is the length of the doctor blade, and U is the casting velocity.⁵ The ratio of the pressure force to shear force determines the flow characteristics and the wet tape thickness for tape casting. Since a viscous force is more favorable than a pressure force for particle alignment, variations to the tape casting process that gives lower Π values should result in a higher degree of texture.⁵

In the present study, lead metaniobate ceramics were tape cast with acicular seed particles that serve as templates for subsequent grain growth with a preferred orientation. Lead metaniobate is a ferroelectric ceramic that is isostructural with orthorhombic tungsten bronze where the polar axis is parallel to the crystallographic b -direction.⁶ When subjected to an electric field, the material develops a b -type texture relative to the poling direction.⁷ Previous researchers have shown that the relatively weak piezoelectric response of lead metaniobate can be increased by processing the ceramic with preferred orientation prior to electrical poling.^{1,8} Granahan and co-workers showed that the piezoelectric properties could be improved by tape casting lead metaniobate slurries containing acicular seed particles.¹ However, the effects of tape casting itself on the orientation developed have not been examined with systematic consideration of tape casting variables. In this study, preferred orientation developed through a tape casting process similar to Granahan's will be examined. The link between tape casting variables including variations in seed particle concentration, slurry viscosity, and casting velocity will be linked to varia-

* Corresponding author. Tel.: +1 765 494 4096; fax: +1 765 494 1204.
E-mail address: kbowman@ecn.purdue.edu (K. Bowman).

tions in the degree of preferred orientation developed during processing.

2. Experimental procedure

2.1. Tape casting with acicular seed particles

Acicular seed particles were grown from a melt following the method proposed by Li and co-workers for lead metaniobate of the stoichiometry PbNb_2O_6 .⁹ These particles (Fig. 1) are single crystals of orthorhombic lead metaniobate with an elongated “box” shape. The long axis of these particles is parallel to the crystallographic c -axis with the a - and b -axes parallel to the shorter sides. The ceramic powder used was unfired K81 (Piezo Technologies, Indianapolis, IN). K81 is a modified lead metaniobate, which contains a modest amount of an alkali dopant. When fired, the crystal structure exhibits the ferroelectric, orthorhombic structure with elongated a - and b -axes relative to the c -axis (a : 17.63 Å, b : 17.92 Å, and c : 3.87 Å).

Two generalized slurries based on tape casting of PZT were used in this study. The two slurry compositions are shown in Table 1.¹⁰ The solvent used was a 67/33 by weight mixture of methyl ethyl ketone (M209-4, Fisher Scientific, Waltham, MA) and ethanol (A407-4, Fisher Scientific, Waltham, MA). The binder and plasticizer used were polyvinyl butyral (Butvar B-98, Tape Casting Warehouse, Yardley, PA) and butyl benzyl phthalate (S-160, Tape Casting Warehouse, Yardley, PA), respectively. In addition, two different dispersants were used. Slurries designated PE employed a phosphate ester dispersant

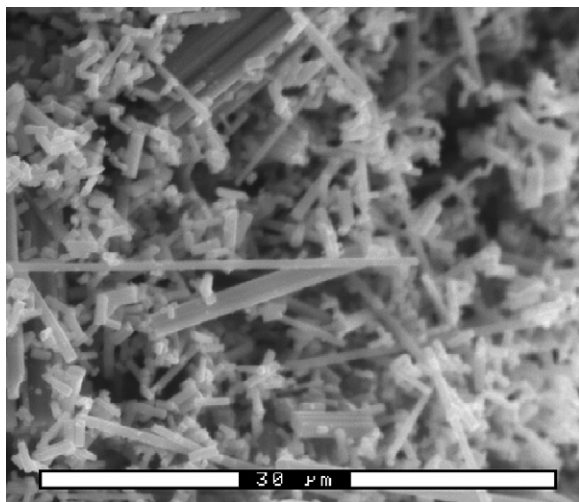


Fig. 1. SEM micrograph of PbNb_2O_6 acicular seed particles grown from a molten salt synthesis procedure. The particles are of a PbNb_2O_6 stoichiometry with the long axis parallel to a crystallographic c -direction.

Table 1
Breakdown of the PE and HYP slurries used in the present study

	Ceramic	Solvent	Binder	Plasticizer	Dispersant
PE	64.7	22.4	5.7	6.7	0.5
HYP	65.8	22.8	4.1	6.8	0.5

Numbers are given in wt%.

(PE-1168, Huntsman, The Woodlands, TX) while slurries designated HYP used hypermer KD-1 dispersants (KD-1, Tape Casting Warehouse, Yardley, PA).

The powder (K81), solvent, and dispersant were ball milled for 24 h, at which time the binder and plasticizer were added. This mixture was then ball milled for 23 h, followed by the incorporation of the required amount of seed particles. After 1 h of ball milling, the slurry was de-aired under vacuum. Slurry viscosities were measured using a Brookfield viscometer (Dial Reading Viscometer, Brookfield Engineering, Middleboro, MA) over a range of shear rates. The equivalent shear rate is calculated using the spindle size and speed accompanied with conversion information provided from the manufacturer.

Seed particle concentrations were varied by weight of K81 powder. The HYP slurries were cast with concentrations of 0, 5, 10, 15, and 20 wt% seed particles. The PE slurry was cast solely with 5 wt% seed particles. Casting velocities were 20 and 80 cm/min for the HYP slurries containing 10 wt% seed particles. All other slurries were cast at a velocity of 20 cm/min. After casting, tapes were dried for 24 h at room temperature. Green tapes were cut and laminated into stacks of 10–20 sheets. Care was taken to keep the orientations of the green tapes consistent during lamination. Laminates were pressed at 6.9 MPa with heated platens at 38 °C. After lamination, samples were bisque fired and sintered at 600 and 1240 °C, respectively.

2.2. Texture evaluation from diffraction experiments

Directions discussed in this paper are designated as the tape casting direction (TCD), tape casting normal (TCN), and transverse direction (TD), shown in Fig. 2. After firing, samples were polished to a fine grit (1 μm) on the tape cast normal (TCN). To examine texture, two diffraction experiments were employed. Cu Kα X-ray diffraction (D500, Siemens, Germany) was performed over an angular range of 20–50° in 2θ to examine differences in the diffraction patterns relative to a random sample. X-ray diffraction patterns taken on the TCN of each sample were used to quantify the development of preferred orientation using the Lotgering factor.¹¹ Accounting for the a - b texture occurring during layered manufacturing of lead metaniobate, Hagh and coworkers proposed the equation:

$$f = \frac{p_{\text{tex}} - p_o}{1 - p_o} \times 100, \quad p_{\text{tex}} = \frac{\sum I_{hk0}}{\sum I_{hkl}} \quad (2)$$

to quantify the a - b texture arising during texture processing.⁸ However, significant peak overlap inhibits the use of all of the

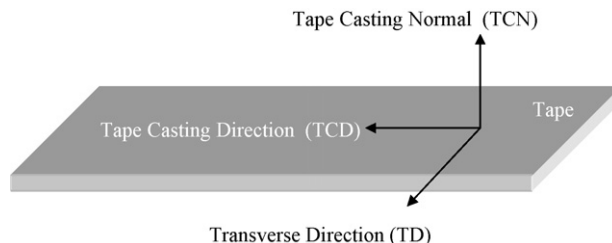


Fig. 2. Directions relative to the present tape casting setup.

peaks occurring in this angular range. For this study, the integrated intensities of the crystallographic peaks highlighted in Fig. 4 on an unpoled, random K81 sample were used to quantify the Lotgering factor using Eq. (2).

While the Lotgering factor can be used to quantify texture, only one sample orientation is examined. In lead metaniobate, multiple peaks in the X-ray diffraction spectra overlap and the textures developed during tape casting develop an orthorhombic symmetry relative to the sample.⁷ Texture methods that examine the full sample orientation space are more beneficial when examining lead metaniobate. A more rigorous and complete method for quantifying texture is the calculation of an orientation distribution function (ODF). To do this, neutron diffraction was employed using the High Pressure Preferred Orientation Diffractometer (HIPPO) at the Los Alamos National Laboratory.¹² The details of the experiment are identical to those described in prior work.⁷ Second-order spherical harmonic coefficients were refined as part of a Rietveld refinement of the neutron time-of-flight diffraction patterns using the program, Materials Analysis Using Diffraction (MAUD).^{13–16} The lead metaniobate model used in this study was refined from an unpoled K81 standard beginning with the model proposed by Labbe and coworkers.¹⁷ With this method, crystallographic information is obtained from the entire sample orientation space. Pole figures were centered on the 001 pole figure minima with the 001 maximum fixed at the pole figure ‘north’ and ‘south’ poles. The pole figure geometry relative to each pole figure is also given.

3. Results and discussion

3.1. Calculating the Π value

Fig. 3 shows a comparison between the viscosities of the HYP and PE slurries containing 5 wt% of seed particles as a function of shear rate. The PE slurries are more viscous at all shear rates. Both slurries exhibit shear thinning behavior as the viscosities decrease as a function of shear rate. This is nontrivial as the viscosity during casting is used to quantify the Π value. A power law equation is fit to the data in order to calculate equivalent viscosities for shear rates, which could not be directly measured. The equations take the form:

$$\eta = 13.5 \times \dot{\gamma}^{-0.30} \quad (3)$$

and

$$\eta = 5.1 \times \dot{\gamma}^{-0.24} \quad (4)$$

Table 2

Values used in quantifying the Π value

Pressure driven values		Shear-driven values used		Π values	
ρ_{slurry}	2288 kg/m ³	L	6.46×10^{-3} m	Π_{PE}	0.040
g	9.8 m/s ²	U	20 cm/min	$\Pi_{\eta_{\text{HYP}2.8}}$	0.093
H_{slurry}	5.5×10^{-3} m	Shear rate	11.11 s ⁻¹	$\Pi_{\eta_{\text{HYP}2.0}}$	0.033
H	300×10^{-6} m	η_{PE}	6.5 Pa s		
$\Delta P \cdot H^2$	8.635×10^{-6} N	η_{HYP}	2.8 Pa s	2.0 Pa s	

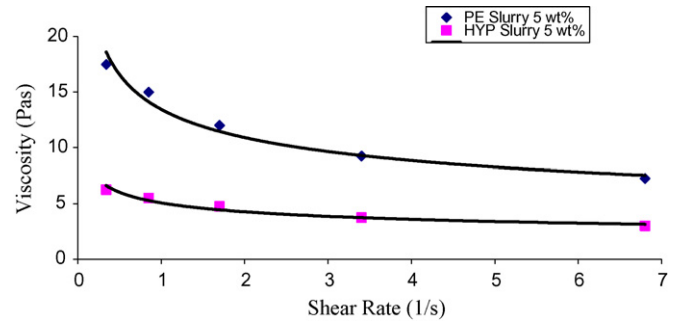


Fig. 3. Viscosity profiles for the two slurries used in this study. The PE slurry has a higher viscosity at all shear rates than the HYP slurry. Using the equations fit to the data points, viscosity values can be estimated for shear rates, which cannot be directly measured.

where η is given in Pa s and $\dot{\gamma}$ is given in s⁻¹ for the PE and HYP slurries, respectively.

An approximation of the shear rates developed in the slurry as a function of casting velocity is taken as simply the casting velocity over the blade gap.

The values used to quantify the Π values for the PE slurry and the three casting velocities of the HYP slurries are shown in Table 2. The equivalent viscosities for the shear rates in question were extracted from the viscosity data trend line. This is a reasonable method as the shear rates calculated occur in the linear region of the viscosity profile. The value for slurry density was calculated by examining the mixed density present from only the starting powder (6.6 g/cm³) and solvent (0.8 g/cm³). The height of the slurry was measured from the slurry mark left on the backside of the doctor blade after casting. The thickness of the single blade device used was 6.46 mm. All other values were fixed by the geometry of the experiment.

In all of the slurries used in this paper, the calculated Π value is below unity. This indicates that in the system examined, shear-driven behavior dominates the flow behavior of the slurry regardless of the casting parameters. Still, altering the tape casting conditions of slurry viscosity and casting velocity does have an effect on the calculated Π value. For the low viscosity (HYP) slurry, as the casting velocity is increased from 20 to 80 cm/min, the Π value decreases from 0.093 to 0.033. By comparison, the Π value for the high viscosity (PE) slurry 0.040 approaches the value calculated for the low viscosity (HYP) slurry at the elevated casting rate. This indicates that although the flow behavior is dominated by viscous forces during casting, the magnitude of shear-driven forces can still be increased by increasing the casting velocity or increasing the slurry viscosity independent of one another.

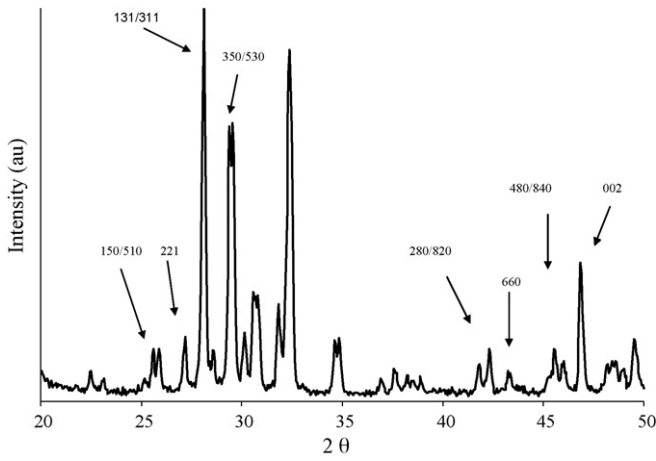


Fig. 4. Cu K α diffraction pattern for unpoled, random K81 lead metaniobate ceramic. Indexed on the pattern are the specific crystallographic peaks, which were used to quantify texture, using the Lotgering factor.

3.2. Texture evaluation from X-ray diffraction

Fig. 4 shows a diffraction pattern for an unpoled, random K81 sample. Indexed on this pattern are the peaks used to identify crystallographic textures in lead metaniobate. As explained in a prior work, peaks that have components relative to only an a - or b -direction (010, 100, etc.) are either low in intensity or overlap other peaks in the diffraction spectra.¹⁸ However, there are multiple sets of peak ‘doublets’ which have fractionalized components relative to the a -, b -, and c -directions. Several of these peaks are difficult to resolve and are simply identified by their composite ‘doublet’. The development of crystallographic texture can be quantified by examining differences in relative intensity for peaks containing no c -axis component, a mixture of a -, b -, and c -components, and only c -components. Of the peaks identified in a random sample, the 131/311 doublet has the highest relative intensity for any peak in the diffraction spectra for random lead metaniobate. The 002 peak has the highest relative intensity for any peak containing only a c -type component. The 350/530 peak doublet has the highest relative intensity for any peak containing only a - and b -components.

Figs. 5–7 show a collection of X-ray diffraction patterns taken on the TCN of tape cast samples as a function of seed particle concentration, casting velocity, and slurry viscosity, respectively. As the seed particle concentration, casting velocity, and slurry viscosity is increased, the intensity of peaks with no c -component ($hk0/kh0$ peaks) increases relative to peaks that have c -components ($hkl, 00l$), indicating that a preferred a – b -texture develops relative to the TCN. The shear behavior of the slurry acts to align the long axis of the seed particles parallel to the TCD. With the long axis of the particles parallel to a crystallographic c -direction, a - and b -textures are expected to develop normal to the TCD. As the concentration of seed particles increases, the number of templates for anisotropic grain growth increases resulting in the increased a - and b -texture. As the casting velocity or slurry viscosity increases, the amount of shear-driven flow increases, indicated by the decreasing Π values. With the increased shear-driven flow, greater particle

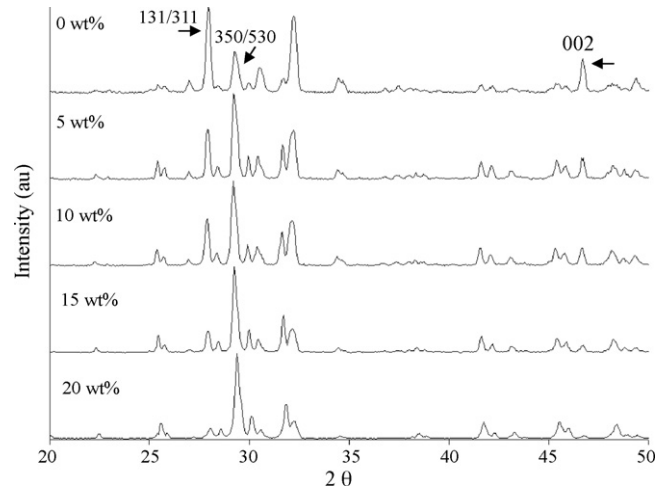


Fig. 5. X-ray diffraction patterns on the TCN for the low viscosity (HYP) slurries cast at 20 cm/min as a function of seed particle concentration. As the seed particle concentration is increased, peaks, which have components only relative to a crystallographic a - or b -direction, increase in intensity while all other peaks in the diffraction pattern decrease in intensity.

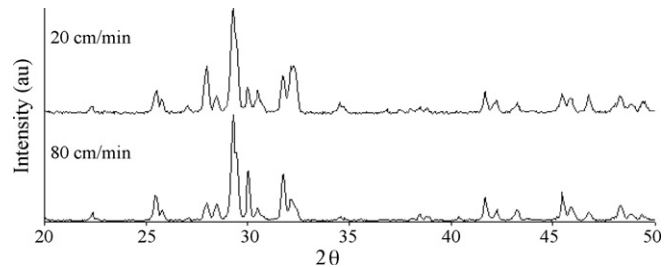


Fig. 6. X-ray diffraction patterns on the TCN of two laminates containing concentrations of 10 wt% of seed particles cast at two different velocities. In both cases, peaks, which have no component relative to a c -direction, are increased in intensity relative to a random sample. However, increasing the casting velocity from 20 to 80 cm/min further increases the intensity of $hk0$ type peaks.

orientation occurs as evidenced by the increase in intensity for $hk0$ type peaks relative to the TCN, and the decrease in intensity for peaks having a c -type component. Using Fig. 7, when the template concentration is identical the increase in intensity is more dramatic for the high viscosity slurry. From the Π values, at equal casting velocities, the high viscosity slurry has a larger component of shear-driven flow than the low viscosity slurry.

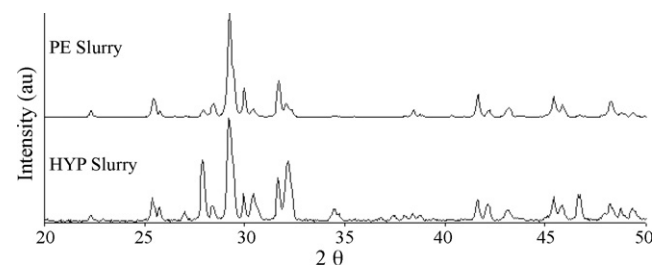


Fig. 7. X-ray diffraction patterns on the TCN of two laminates containing concentrations of 5 wt% of seed particles cast from two slurries with different viscosities. In both cases, peaks, which have no components relative to a c -direction, are increase in intensity relative to a random sample. However, the increased slurry viscosity found in the PE slurry resulted in a much more drastic increase.

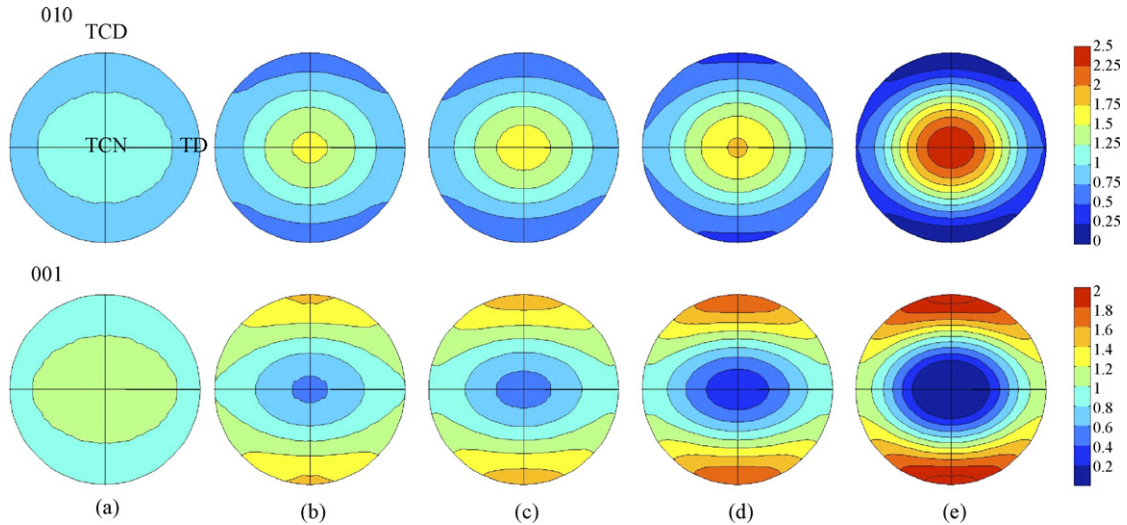


Fig. 8. 010 and 001 pole figures for the low viscosity slurries cast with varying seed particle concentrations. Figures (a)–(e) correspond to 0, 5, 10, 15, and 20 wt%, respectively. As the seed particle concentration increases, the 010 texture increases relative to the sample TCN and the 001 texture increases relative to the sample TCD.

This equates to more particle rotation and orientation resulting in an increase in texture without an increase in seed particle concentration.

The degree of preferred orientation can be quantified using the integrated intensities of the diffraction patterns in Figs. 4–7 combined with Eq. (2). Table 3 lists the calculated Lotgering factors for each of the tape casting conditions used. As the seed particle concentration, casting velocity, or slurry viscosity is increased, the quantified degree of preferred orientation increases from a value of roughly 1.5% for the HYP slurry containing no templates to a maximum value of greater than 84% for the high viscosity slurry containing 5 wt% of templates.

3.3. Texture quantification from neutron diffraction

Table 3 also summarizes the 010 and 001 pole figure maxima for all of the tape casting experiments used in this research. Fig. 8 shows the 001 and 010 pole figures for the low viscosity slurries cast with seed particle concentrations of 5, 10, 15, and 20 wt%. From Table 2, the expected Π value for these slurries remains constant at 0.093. As the seed particle concentration increases, the maximum 001 pole density increases in the TCD and decreases in the TCN and TD. Conversely, 010 textures increased in the TCN with a decrease in the TCD and TD. This

indicates an increase in both 010 and 001 type textures as a function of seed particle concentration.

Fig. 9 shows a comparison between pole figures for samples containing 5 wt% seed particles for the high and low viscosity slurries. The higher viscosity slurry allows for increased 010 and 001 pole densities using a smaller fraction of seed particles. This results from an increased slurry viscosity and a larger shear force during tape casting. As indicated by the differing Π values (0.093 for the HYP slurry, 0.040 for the PE slurry), there is an increased shear force resulting in more particle rotation and subsequent preferred orientation.

Increasing the casting velocity also increases the magnitude of shear forces during deformation. Fig. 10 shows the 010 and 001 pole figures calculated from the low viscosity slurry for seed particle concentrations of 10 wt% at casting velocities of 20 and 80 cm/min. There is an increase in maximum pole density of

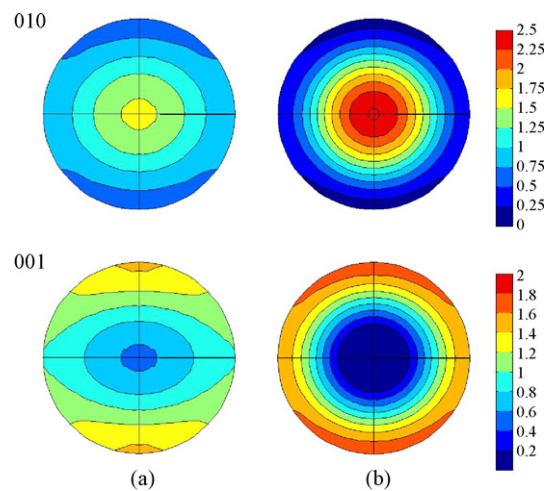


Fig. 9. 010 and 001 pole figures for the high (b) and low (a) viscosity slurries containing seed particle concentrations of 5 wt%. In both cases, 010 and 001 textures increase relative to the TCN and TCD, respectively, but in the high viscosity case, there is a greater increase in texture.

Table 3
Lotgering factors and MRD values for all of the tape casting conditions

	Cu K α , Lotgering	Neutron	
		010 MRD	001 MRD
HYP 0	1.56	1.15	1.16
HYP 5	41.25	1.55	1.37
HYP 10	52.99	1.62	1.43
HYP 15	66.78	1.78	1.68
HYP 20	72.59	2.49	1.96
HYP10 4X	78.09	1.89	1.64
PE 5	84.25	2.52	1.70

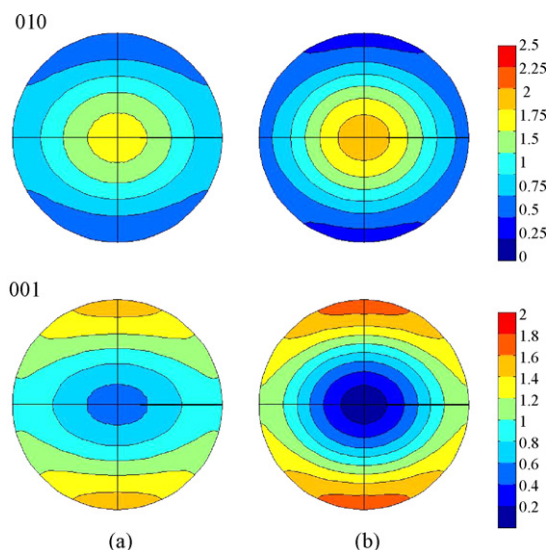


Fig. 10. 010 and 001 pole figures for laminates containing seed particle concentrations of 10 wt% cast at 20 cm/min (a) and 80 cm/min (b). In both cases, 010 and 001 textures increase relative to the TCN and TCD, respectively, but in the laminate cast at 80 cm/min, there is a greater increase in texture.

both the 010 and 001 pole figures when using the higher casting velocity. This is due to an increase in shear-driven deformation with casting velocity quantified using the Π values of 0.093 at 20 cm/min and 0.033 at 80 cm/min.

This research has shown that the development of preferred orientation from tape casting is sensitive to the slurry properties and the tape casting conditions. While care has been taken to test systematically the effects of casting velocity, slurry viscosity, and template concentration, some of the results suggest that these variables are not necessarily independent of one another. While viscosity is dependent on the casting velocity due to the shear thinning behavior exhibited by all of the slurries, the seed particle concentration may also have an effect on the slurry rheology. When calculating the Π value, slurry rheology is assumed to be fixed depending on whether the slurry used is high viscosity or low viscosity. When comparing two slurries cast with identical template concentrations and viscosity profiles, the assumption that decreasing the Π value alone will increase texture appears to hold. The HYP slurries with 10 wt% templates cast at 20 and 80 cm/min (Fig. 10a and b, respectively) showed both an increase in texture and a decrease in calculated Π value as a function of casting velocity. Similar behavior is observed when comparing slurries with identical template concentrations, but different viscosity profiles. Comparing the HYP and PE slurries containing 5 wt% templates (Fig. 9a and b, respectively), as the viscosity is increased, the Π value decreases and the textures increases.

As previous researchers have shown, simply increasing the template concentration will lead to an increase in texture. However, increasing the template concentration may inadvertently alter the slurry rheology. This becomes an issue when comparing the effects across variations in slurry viscosity, casting velocity, and template concentration. For instance, the highest 010 textures achieved occurred using the PE slurry with a tem-

plate concentration of 5 wt%. The calculated Π value in this case is 0.040. By comparison, the calculated Π value for the HYP slurry cast at 80 cm/min with a template concentration of 10 wt% is 0.033. The increased seed concentration and lower Π value would both suggest an increase in texture. However, the 010 texture is lower in the HYP slurry than in the PE slurry. Furthermore, the HYP slurry containing 20 wt% of templates has a higher Π value (0.093) than either the PE 5 wt% (0.040) or the HYP 10 wt% at 80 cm/min (0.033) but a higher degree of 010 texture than the HYP 10 wt% slurry cast at 80 cm/min and a higher 001 texture measured across all variations. This indicates that simply increasing the seed particle concentration does not represent a fair comparison between slurries. However, comparisons between slurries with a consistent template concentration but different viscosity profiles or casting velocities, or slurries with identical viscosity profiles but different template concentrations can be compared directly by examining the shear behavior of the slurry.

4. Conclusions

Increases in seed particle concentration, casting velocity, and slurry viscosity all have an effect on the degree of texture induced from tape casting lead metaniobate with acicular seed particles. With an increased seed particle concentration, there will be an increase in the amount of seeds available for anisotropic grain growth. As shown by the low Π value, shear flow will dominate particle orientation even at lower slurry viscosities and casting velocities. Even with low concentrations of seed particles, some particle orientation occurs resulting in the development of preferred orientation. An increased seed particle concentration increases the number of templates that become oriented during casting. With more particles available, more particles become oriented prior to firing and larger degrees of texture are achieved.

When the Π value is decreased, either by increasing the slurry viscosity or increasing the casting velocity, the shear behavior of the slurry is increased. This allows for more particle rotation and orientation and the development of greater textures. Although samples cast with low concentrations of seed particles do develop preferred orientation, the amount of preferred orientation can be increased by either increasing the slurry viscosity or increasing the casting velocity independently.

Acknowledgements

This work was supported by the National Science Foundation, DMR – 0224991. Materials and assistance were provided by Piezotechnologies, Indianapolis, IN.

References

1. Granhan, M., Holmes, M., Schulze, W. A. and Newham, R. E., Grain-oriented PbNb_2O_6 ceramics. *J. Am. Ceram. Soc.*, 1981, **64**(4), C68–C69.
2. Duran, C., Trolier-McKinstry, S. and Messing, G. L., Dielectric and piezoelectric properties of textured $\text{Sr}_{0.53}\text{Ba}_{0.47}\text{Nb}_2\text{O}_6$ ceramics prepared by templated grain growth. *J. Mater. Res.*, 2003, **18**, 228–238.

3. Jing, X., Li, Y., Yang, Q., Zeng, J. and Yin, Q., Influence of different templates on the textured $\text{Bi}_{0.5}(\text{Na}_{1-x}\text{K}_x)_{0.5}\text{TiO}_3$ piezoelectric ceramics by the reactive templated grain growth process. *Ceram. Int.*, 2004, **30**, 1889–1893.
4. Seabaug, M. M., Cheney, G. L., Hasinska, K., Azad, A.-M., Sabolsky, E. M., Swartz, S. L. et al., Development of a templated grain growth system for texturing piezoelectric ceramics. *J. Int. Mater. Syst. Struct.*, 2004, **15**, 209–214.
5. Kim, H. J., Krane, M. J. M., Trumble, K. P. and Bowman, K. J., Analytical fluid flow models for tape casting. *J. Am. Ceram. Soc.*, 2006, **89**(9), 2769–2775.
6. Francombe, M. H. and Lewis, B., Structural, dielectric and optical properties of ferroelectric lead metaniobate. *Acta Crystallogr.*, 1958, **11**, 696–703.
7. Iverson, B., Jones, J. L. and Bowman, K. J., Neutron texture assessment of ferroelectric lead metaniobate. *Phys. B: Condens. Matter*, 2006, **385/386**(1), 581–583.
8. Hagh, N. M., Nonaka, K., Allahverdi, M. and Safari, A., Processing-property relations in grain-oriented lead metaniobate ceramics fabricated by layered manufacturing. *J. Am. Ceram. Soc.*, 2005, **88**(11), 3043–3048.
9. Li, C. C., Chiu, C. C. and Desu, S. B., Formation of lead niobates in molten-salt systems. *J. Am. Ceram. Soc.*, 1991, **74**(1), 42–47.
10. Galassi, C., Roncari, E., Capiani, C. and Pinasco, P., PZT-based suspensions for tape casting. *J. Eur. Ceram. Soc.*, 1997, **17**(2/3), 367–371.
11. Lotgering, F. K., Topotactical reactions with ferromagnetic oxides having hexagonal crystal structures. *J. Inorg. Nucl. Chem.*, 1959, **9**, 113–123.
12. Matthies, S., Pehl, J., Wenk, H.-R., Lutterotti, L. and Vogel, S. C., Quantitative texture analysis with the HIPPO neutron TOF diffractometer. *J. Appl. Crystallogr.*, 2005, **38**(3), 462–475.
13. Rietveld, H. M., A profile refinement method for nuclear and magnetic structures. *J. Appl. Crystallogr.*, 1969, **2**, 65.
14. Matthies, S., Lutterotti, L. and Wenk, H. R., Advances in texture analysis from diffraction spectra. *J. Appl. Crystallogr.*, 1997, **30**, 31–42.
15. Lutterotti, L., Matthies, S. and Wenk, H.-R., MAUD (materials analysis using diffraction): a user friendly Java Program for Rietveld texture analysis and more. In *Proceedings of the International Conference on Textures of Materials (ICOTOM)*, 1999, pp. 1599–1604.
16. The MAUD Program. <http://www.ing.unitn.it/~maud/>.
17. Labbe, P. P., Frey, M. and Allais, G., Nouvelles données structurales sur la variété ferroélectrique du metaniobate de plomb PbNb_2O_6 . *Acta Crystallogr.*, 1973, **B29**, 2204–2210.
18. Key, T. S., Jones, J. L., Shelley, W. F., Iverson, B. J., Li, H. Y., Slamovich, E. B. et al., Texture and symmetry relationships in piezoelectric materials. *Mater. Sci. Forum*, 2005, **495/497**, 13–22.